Physics – Uspekhi **68** (5) 512 – 524 (2025)

INSTRUMENTS AND METHODS OF INVESTIGATION PACS number: 85.70.Sq

Magnetically controlled spin light-emitting diode

M.V. Dorokhin, M.V. Ved', P.B. Demina, Yu.M. Kuznetsov, A.V. Kudrin, A.V. Zdoroveyshchev, D.A. Zdoroveyshchev, N.V. Baidus, I.L. Kalentyeva

DOI: https://doi.org/10.3367/UFNe.2025.03.039886

Contents

Abstract. The fundamental physical principles underlying the operation of basic elements of spintronics are considered, including the giant magnetoresistance effect, injection of spin-polarized charge carriers from a magnetized ferromagnetic contact, and radiative recombination in semiconductors involving spin-polarized carriers. An integrated GaAs-based structure implementing all of the above phenomena, a magnetoresistive spin light-emitting diode, has been fabricated and investigated. As an electrical circuit, the device under consideration is a magnetoresistive element and a metal/tunnel-thin dielectric/semiconductor light-emitting diode connected in series. It is shown that a magnetic field directed in the plane of the layers changes the state of the magnetoresistive element (high or low resistance) and thus allows controlling the intensity of electroluminescence. A magnetic field directed perpendicular to the plane of the layers ensures magnetization of the magnetic contact of the light-emitting diode and spin injection, accompanied by the emission of circularly polarized light. The resulting device can find itself in four stable magnetic states (high-low intensity, 'positive'–'negative' circular polarization). Such a structure can serve as a basis for magnetic recording and information transmission elements, in which four stable states form quaternary instead of binary logic.

Keywords: spintronics, spin injection, spin transport, magnetically controlled LEDs, spin light-emitting diodes, magnetoresistive elements

M.V. Dorokhin [(a)], **M.V. Ved'** [(b)], **P.B. Demina** [(c)], **Yu.M. Kuznetsov** [(d)], **A.V. Kudrin** [(e)], **A.V. Zdoroveyshchev** [(f)], **D.A. Zdoroveyshchev** [(g)], **N.V. Baidus** [(h)], **I.L. Kalentyeva** [(i)]
Lobachevsky State University,
prosp. Gagarina 23, 603022 Nizhny Novgorod, Russian Federation
E-mail: [(a)]dorokhin@nifti.unn.ru, [(b)]ved@nifti.unn.ru, [(c)]demina@phys.unn.ru, [(d)]yurakz94@list.ru, [(e)]kudrin@nifti.unn.ru, [(f)]zdorovei@nifti.unn.ru, [(g)]daniel.zdorov@gmail.com, [(h)]bnv@nifti.unn.ru, [(i)]istery@rambler.ru

Received 3 September 2024, revised 22 January 2025
Uspekhi Fizicheskikh Nauk **195** (5) 543 – 556 (2025)
Translated by V.L. Derbov

1. Introduction

Structures of semiconductor and metallic spintronics are considered as one of the options for developing modern micro- and optoelectronics. Such structures use new principles of information transmission, storage, and processing to overcome fundamental quantum limitations on the number of elements in an integrated circuit [1]. These principles are based on the electron spin, which can take two values (conventionally designated as $+1/2$ and $-1/2$). In 'classical' semiconductors and nonferromagnetic metals, without external influences, the concentrations of free electrons with spins $+1/2$ and $-1/2$ coincide. By creating multilayer magnetic structures or by means of external influences, a situation can be realized when the concentrations of carriers with spins $+1/2$ and $-1/2$ differ. This state is called 'spin polarization of carriers.' In spin-polarized materials, a variety of phenomena associated with spin polarization (spin-dependent phenomena) is observed. These phenomena include the emission of circularly polarized light [2, 3], the spin Hall effect [4], and spin-dependent transport in structures with magnetic inclusions [5, 6]. Several semiconductor devices for electronics and optoelectronics were proposed based on spin-dependent phenomena. Some of the earliest were the Datta and Das

spin field-effect transistor [7], the spin light-emitting diode (SLED) [3], and the 'nonlocal spin valve' transistor [8, 9]. These technical solutions were intended to improve the performance of electronic devices by using new physical principles for storing and transmitting information. Information was contained in the sign of the spin polarization of charge carriers, and spin-dependent phenomena ensured the transformation of spin polarization into an electrical or optical signal and vice versa. The area of science dealing with devices based on spin-dependent phenomena is called spintronics. Although many technical solutions in spintronics are subject to criticism [10, 11], there is no doubt that the complex of spin-dependent phenomena is of fundamental scientific interest and can be used to design auxiliary elements of micro- and optoelectronics [12]. The development of spintronic technologies and the expansion of the functional capabilities of elements based on them include monolithic integration of spintronics devices with classical microelectronic and optoelectronic devices, as well as the unification of various spintronic units in a single device. Such integration will allow the use of additional degrees of freedom in the design of magnetooptical and magnetoelectronic circuits.

This paper presents a review of spin-dependent phenomena that form the basis of two basic elements of spintronics, namely, a spin light-emitting diode (an element that implements the principle of electric injection of spin-polarized carriers into a semiconductor from a magnetized ferromagnetic electrode) and a magnetoresistive element (an element that implements the principle of spin-dependent electron transport). The technical implementation of these devices is reported, as is their functional integration in a film integrated circuit (magnetoresistive spin light-emitting diode). The results of an experimental study of magnetoresistive spin light-emitting diode operation are presented, and the possibility of independent control of magnetoresistive characteristics is demonstrated.

2. Theory

2.1 Principle of spin injection for creating spin-polarized charge carriers

The basic operation for the functioning of devices based on spin-dependent effects is the creation of spin polarization of charge carriers [13]. The degree of spin polarization P_n is quantitatively determined by the relation

$$P_n = \frac{n_+ - n_-}{n_+ + n_-} \times 100\% \,, \tag{1}$$

where n_+ and n_- are the concentrations of charge carriers with spin up and spin down, respectively. To create a nonzero spin polarization in nonferromagnetic materials, external action is required (otherwise, the spin polarization is zero).

There are various methods for creating nonequilibrium spin polarization in a semiconductor [2, 3, 13], e.g., placing a semiconductor in a strong magnetic field, optical generation of charge carriers by pumping with circularly polarized light, and polarization of carriers due to interaction with a nearby ferromagnetic layer. Nevertheless, from the point of view of practical applications, the most promising method for creating nonequilibrium spin polarization in semiconductors is the injection of spin-polarized carriers from a magnetized ferromagnetic material. The theoretical possibility of spin injection from a ferromagnetic metal into a nonferromagnetic semiconductor was demonstrated by Aronov and Pikus in 1976 [14].

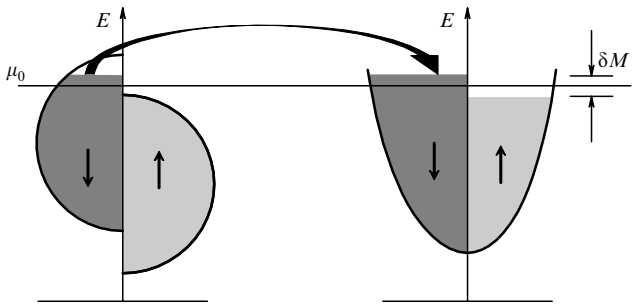

Figure 1. Band diagram of ferromagnetic metal–semiconductor contact with injection of 100% spin-polarized electrons.

Let us consider the physical principles of spin injection in contact between a metallic ferromagnet and a nonferromagnetic material located in an external magnetic field (Fig. 1). For definiteness, we consider the injection of spin-polarized electrons. When spin-polarized holes are injected, all the relations given below are valid, considering the sign of the hole charge. Spin injection of holes was demonstrated experimentally, e.g., in Ref. [15].

The injection of charge carriers from a ferromagnet is implemented by applying an electric bias. As a result of magnetization of the ferromagnet, a preferential equilibrium spin polarization of carriers arises in it, the value of which is denoted by P_n^M. When conditions for electric injection from the ferromagnet into the semiconductor are created, a current of spin-polarized carriers flows in the system, whose degree of polarization is determined as

$$\alpha(z) = \frac{j_\uparrow(z) - j_\downarrow(z)}{j_\uparrow(z) + j_\downarrow(z)} \,, \tag{2}$$

where $j_\uparrow(j_\downarrow)$ are the currents of carriers with spin up (down), and z is the distance from the ferromagnet/semiconductor boundary in the direction of current flow.

The electric current for carriers with different spins depends on the external electric field **E** and on the deviation of the carrier density from the equilibrium value $\delta n_{\uparrow\downarrow}$. We write the drift-diffusion equations,

$$\mathbf{j}_{\uparrow\downarrow} = \sigma_{\uparrow\downarrow}\mathbf{E} - eD_{\uparrow\downarrow}\nabla\delta n_{\uparrow\downarrow} \,, \tag{3}$$

where $\sigma_{\uparrow\downarrow}$ is the electrical conductivity, and $D_{\uparrow\downarrow}$ is the diffusion coefficient. If we introduce the total current $j = j_\uparrow + j_\downarrow$ and the spin current $j_s = j_\uparrow - j_\downarrow$, then Eqn (2) can be rewritten as

$$\alpha = \frac{j_s}{j} \,. \tag{4}$$

Keeping in mind that $\delta n_{\uparrow\downarrow} = N_{\uparrow\downarrow}\delta\varepsilon_F^{\uparrow\downarrow}$, where $N_{\uparrow\downarrow}$ is the density of states on the spin subbands and $\delta\varepsilon_F^{\uparrow\downarrow}$ is the shift of the Fermi energy from the equilibrium state, and using the relation $\sigma_{\uparrow\downarrow} = e^2 N_{\uparrow\downarrow} D_{\uparrow\downarrow}$, the expressions for the currents of carriers with spin up and down can be written as

$$\mathbf{j}_\uparrow = \sigma_\uparrow \nabla\mu_\uparrow \,, \qquad \mathbf{j}_\downarrow = \sigma_\downarrow \nabla\mu_\downarrow \,, \tag{5}$$

where $\mu_{\uparrow\downarrow} = \varepsilon_F^{\uparrow\downarrow}/e - \varphi$ is the electrochemical potential (ECP), and φ is the electric potential. From Eqn (4), it follows that

the spin current j_s is caused by the difference among electrochemical potentials for carriers with different spin values. We introduce the average value of the electrochemical potential $\mu = (\mu_\uparrow + \mu_\downarrow)/2$ and the difference between electrochemical potentials for carriers with spins up and down $\mu_s = \mu_\uparrow - \mu_\downarrow$.

The continuity equation requires the following relationships to be satisfied:

$$\nabla(\mathbf{j}_\uparrow + \mathbf{j}_\downarrow) = 0\,, \qquad \nabla(\mathbf{j}_\uparrow - \mathbf{j}_\downarrow) = -e\,\frac{\delta n_\uparrow}{\tau_{\uparrow\downarrow}} + e\,\frac{\delta n_\downarrow}{\tau_{\downarrow\uparrow}}\,, \tag{6}$$

where $\tau_{\uparrow\downarrow}(\tau_{\downarrow\uparrow})$ is the time during which an electron is scattered from the spin-up state to the spin-down state (and vice versa). With Eqns (6) and the balance equation $N_\uparrow/\tau_{\uparrow\downarrow} = N_\downarrow/\tau_{\downarrow\uparrow}$ taken into account, it is possible to write

$$\nabla^2(\sigma_\uparrow\mu_\uparrow + \sigma_\downarrow\mu_\downarrow) = 0\,, \tag{7}$$

$$\nabla^2(\mu_s) = \frac{1}{\lambda^2}\,\mu_s\,, \tag{8}$$

where $\lambda = \sqrt{D\tau_{sf}}$ is the spin diffusion length, $\tau_{sf} = (1/2)(\tau_{\uparrow\downarrow} + \tau_{\downarrow\uparrow})$ is the mean time of spin relaxation, and $D^{-1} = (N_\uparrow D_\downarrow^{-1} + N_\downarrow D_\uparrow^{-1})/(N_\uparrow + N_\downarrow)$. The spin diffusion length is an important material property for constructing devices based on spin-dependent effects [13].

In the general form, the solution to Eqn (8) looks like the following:

$$\mu_s = \mu_s(0)\exp\left(-\frac{x}{\lambda}\right). \tag{9}$$

Expression (9) is commonly considered from the side of the ferromagnetic injector and from the side of the semiconductor, respectively:

$$\mu_s^F = \mu_s^F(0)\exp\left(\frac{x}{\lambda_F}\right), \quad \mu_s^N = \mu_s^N(0)\exp\left(-\frac{x}{\lambda_N}\right). \tag{10}$$

It should be considered that the values of the spin diffusion length for a semiconductor (λ_N) and a ferromagnetic metal (λ_F) differ greatly: for metals, it is 5–50 nm; for semiconductors such as GaAs and Si, it is 1–5 μm [13]. From here on, all quantities related to the ferromagnet will have the subscript F, and those related to the nonferromagnetic material (in particular, a semiconductor) will have the subscript N.

We assume the following boundary conditions:

— no spin scattering during carrier transfer across the interface:

$$\alpha^F(-0) = \alpha^N(+0)\,; \tag{11}$$

— the electrochemical potential is not continuous when crossing the interface; the magnitude of the discontinuity is determined by the following boundary condition:

$$j_{\uparrow\downarrow}(0) = \Sigma_{\uparrow\downarrow}\left[\mu_{\uparrow\downarrow}^N(0) - \mu_{\uparrow\downarrow}^F(0)\right], \tag{12}$$

where $\Sigma = \Sigma_\uparrow + \Sigma_\downarrow$ is the contact conductivity. For a ferromagnet/semiconductor contact, $\Sigma_\uparrow \neq \Sigma_\downarrow$. By transforming equations (11) and (12), it can be shown that

$$\mu_s^N(0) - \mu_s^F(0) = 2r_c(\alpha - P_\Sigma)\,j\,, \tag{13}$$

$$\mu^N(0) - \mu^F(0) = r_c(1 - P_\Sigma\alpha)\,j\,, \tag{14}$$

where $r_c = \Sigma/(4\Sigma_\uparrow\Sigma_\downarrow)$ has the meaning of the effective contact resistance and $P_\Sigma = (\Sigma_\uparrow - \Sigma_\downarrow)/(\Sigma_\uparrow + \Sigma_\downarrow)$.

With Eqns (5) taken into account, the degree of spin polarization can be expressed as

$$\alpha = \frac{2(\sigma_\uparrow\sigma_\downarrow/\sigma)\nabla\mu_s}{j} + P_\sigma\,, \tag{15}$$

where $P_\sigma = (\sigma_\uparrow - \sigma_\downarrow)/(\sigma_\uparrow + \sigma_\downarrow)$ is the relative difference between conductivities of spin-up and spin-down channels. It is worth noting that, in a semiconductor material, $P_\sigma = 0$. Considering Eqn (15), we can obtain expressions for the coefficients at the exponential function in Eqn (10) for a ferromagnet and a semiconductor:

$$\mu_s^F(0) = 2r_F(\alpha - P_\sigma)\,j\,, \qquad \mu_s^N(0) = 2r_N\alpha j\,, \tag{16}$$

where $r_F = \lambda_F\sigma_F/(4\sigma_\uparrow\sigma_\downarrow)$ and $r_N = \lambda_N/\sigma_N$ are the effective resistances of the ferromagnet and semiconductor, $\sigma_F = \sigma_\uparrow + \sigma_\downarrow$ is the total conductivity in the spin-up and spin-down channels, and σ_N is the conductivity in the semiconductor.

Thus, by transforming expressions (15) and (16), we can obtain an expression for the degree of spin polarization of the current at the interface between the ferromagnet and the semiconductor:

$$\alpha(0) = \frac{r_c P_\Sigma + r_F P_{\sigma F}}{r_{FN}}\,, \tag{17}$$

where $r_{FN} = r_F + r_c + r_N$ is the effective equilibrium resistance of the ferromagnet/semiconductor contact.

It is worth noting that a high degree of spin polarization of the current in a semiconductor does not generally imply a high value of the degree of spin polarization of carriers P_n, since, according to Ref. [13], in the near-surface region of the semiconductor, $\alpha \neq P_n$. To calculate P_n, Poisson's equations and the quasi-neutrality condition are used.

2.2 Detection of spin polarization of charge carriers in a semiconductor. Spin light-emitting diode

There are several approaches to detecting spin polarization, such as using the magnetooptical Kerr effect with high spatial resolution [16], recording circularly polarized radiation, or studying the magnetoresistive effect. One of the most common methods is recording circularly polarized radiation arising due to recombination transitions of spin-polarized charge carriers [2, 3]. The method is based on the relationship between the spin polarization of charge carriers participating in radiative recombination and the circular polarization of electroluminescence radiation that occurs during the recombination of spin-polarized carriers [2, 3].

Let us consider in more detail the recombination processes involving spin-polarized charge carriers. Assume 100% of spin-polarized electrons are injected from metal to semiconductor (see Fig. 1). In a diode structure, the injected spin-polarized electrons recombine with holes coming from the bulk of the semiconductor, emitting a photon (it is most often assumed that the holes are not spin polarized). The diagram of possible radiative transitions is shown in Fig. 2.

During the process of radiative recombination, a transition of the electron to a hole state occurs, resulting in the creation of a photon. In this case, the laws of conservation of energy, quasi-momentum, and angular momentum must

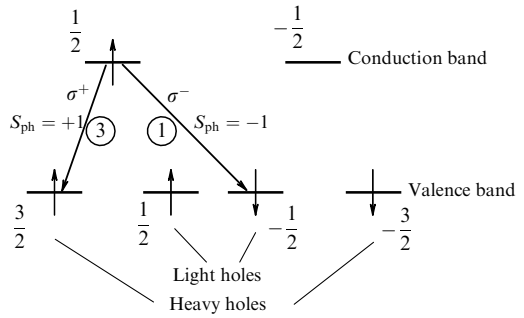

Figure 2. Allowed radiative transitions during recombination of 100% spin-polarized electrons with unpolarized holes in a bulk semiconductor. Fractional numbers denote carrier spins, circled numbers denote transition probabilities. Italics denote spin values (S_{ph}) of photon emitted during corresponding transition.

hold. The law of energy conservation is manifested in the fact that the energy lost by the electron during the transition is transferred to the created photon, which, in accordance with known relationships, determines the energy ΔE, the wavelength λ, and the wave number k of the generated photon:

$$\Delta E = h\nu, \qquad \lambda = \frac{c}{\nu}, \qquad k = \frac{2\pi}{\lambda}, \tag{18}$$

where c is the speed of light, h is the Planck constant, and ν is the frequency of the electromagnetic wave.

At the same time, it is necessary to keep in mind that, in a single recombination event, a single photon is created, which is a quantum particle. Therefore, the properties of the photon should be considered in terms of quantum physics. According to Ref. [17], in the general case, a photon or one-photon electromagnetic field is defined as a linear combination of single-photon states. A single-photon state is that of a harmonic oscillator, which corresponds to a plane monochromatic wave with a wave vector $\mathbf{k}$ and polarization α ($|1_{k,\alpha}\rangle$). Here, α can take two values, corresponding to two mutually perpendicular directions lying in a plane perpendicular to the vector $\mathbf{k}$. The state of the photon is written as

$$|\xi\rangle = \sum_{k,\alpha} b_{k,\alpha}|1_{k,\alpha}\rangle, \tag{19}$$

where $b_{k,\alpha}$ are coefficients satisfying the normalization conditions:

$$\sum_{k,\alpha} b^*_{k,\alpha} b_{k,\alpha} = \sum_{k,\alpha} |b_{k,\alpha}|^2 = 1. \tag{20}$$

Generally speaking, the representation of a photon as a superposition of plane waves is not unique. It is possible to decompose a photon into a set of basis states, which are usually chosen to be most convenient for considering a specific problem. When considering recombination optical transitions, it is convenient to use basis states in the form of spherical waves. In this case, the single-photon states will be characterized by the angular momentum j and parity (j^+ or j^-), rather than by k and α [17]. The total angular momentum of a photon can take values $j = 1, 2, 3, \ldots$ (the state $j = 0$ does not exist for a photon, which follows from the electromagnetic wave transversality condition [17]). The parity of a photon is determined by the behavior of the vector potential $\mathbf{A}(\mathbf{r})$ under inversion of the coordinate system. For a polar vector $\mathbf{A}$, which changes sign under inversion ($\mathbf{A}(-\mathbf{r}) = -\mathbf{A}(\mathbf{r})$), the parity is $+1$, and if $\mathbf{A}(-\mathbf{r}) = \mathbf{A}(\mathbf{r})$, then the parity is -1.

When considering the laws of conservation of angular momentum for an optical transition, as in the previous case, it is convenient to use the expansion in spherical waves. The wave vector $\mathbf{k}$ when calculating optical transitions is included in the matrix element of the transition in the form of a factor $\exp(i\mathbf{kr})$, where $\mathbf{r}$ is the radius vector, drawn from the center of the atom ($0 \leqslant r \lesssim$ atomic radius). For optical transitions, $\mathbf{kr} \ll 1$; therefore,

$$\exp(i\mathbf{kr}) = 1 + i\mathbf{kr} - \frac{1}{2}(\mathbf{kr})^2 + \ldots. \tag{21}$$

Expansion (21) corresponds to the expansion of the $k\alpha$ state in spherical functions. The first term of the expansion corresponds to a spherical function with $j = 1$, the second, to $j = 2$, etc. In the case of optical transitions, we limit ourselves to the first term of the expansion, which is referred to as the dipole approximation. It is the dipole approximation in which optical transitions are considered in Ref. [2], where the basic principles of spintronics are described.

If L is the size of the radiating system and λ is the radiation wavelength, then the ratio of the probabilities of generating photons of different types is written as

$$\frac{W(1^+)}{W(2^-)} \sim \frac{W(1^+)}{W(1^-)} \sim \left(\frac{\lambda}{L}\right)^2. \tag{22}$$

For semiconductors used in optoelectronics, $\lambda \sim 1$ μm, $a \sim 10$ nm (the size of the active region); therefore, $W(1^+)/W(2^-) \sim W(1^+)/W(1^-) \sim 10^4$. In other words, the probability of emitting photons with angular momentum $j = 1$ and parity $(+)$ is many orders of magnitude higher than the probability of all other transitions.

Let us consider the conservation law for the projection of angular momentum in a certain preferred direction. For $j = 1$, the projection of the photon angular momentum is $S_{ph} = \pm 1$. The state $S_{ph} = 0$ is impossible due to the above-mentioned condition of the electromagnetic wave transversality. The value of S_{ph} is sometimes called the photon spin, by analogy with the fact that, for an electron, the projection of the angular momentum onto a preferred direction is also called spin. Thus, during recombination, only those transitions are allowed in which the projection of the angular momentum changes by $+1$ or -1. This angular momentum is transferred to the emitted photon. A diagram of possible optical transitions at 100% polarization of electrons with a change in the projection of angular momentum by ± 1 is shown in Fig. 2. The numbers in the circles in Fig. 2 also indicate the relative transition probabilities introduced in Ref. [2].

Considering the selection rules indicated in Fig. 2, one can propose another basis for decomposing the photon states, namely, the basis of circularly polarized waves:

$$|\xi\rangle = b_1|1_{k,+|S|}\rangle + b_2|1_{k,-|S|}\rangle, \tag{23}$$

where S is the helicity of the photon, i.e., the projection of the angular momentum onto the $\mathbf{k}$ direction. The states with $S > 0$ correspond to a light wave with left-hand circular polarization (σ^+), for which the angular momentum is $+1$, while states with $S < 0$ correspond to a wave with right-hand circular polarization (σ^-) and angular momentum -1.

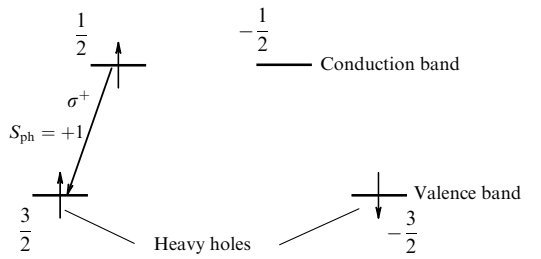

Figure 3. Allowed radiative transitions during recombination of 100% spin-polarized electrons with unpolarized holes in a structure with an elastically strained InGaAs/GaAs quantum well.

Furthermore, if we consider a system of levels that do not contain states of light holes, then the scheme of optical transitions is simplified. Such a system is realized in structures with an elastically strained InGaAs/GaAs quantum well [3]. At 100% spin polarization of electrons, the emission of a photon with only one value of S becomes possible (Fig. 3).

This corresponds to a monochromatic wave with circular polarization. Electromagnetic radiation in the regime of magnetic field-controlled electroluminescence can be considered a superposition of multiphoton states, but, in this case, each single-photon state will be characterized by a circularly polarized wave with $b_1 = 1$ and $b_2 = 0$. A similar situation describes the case of circularly polarized incoherent radiation realized in practice. It can be defined as an electromagnetic wave in which the phase difference between two mutually perpendicular projections of the vector **E** is always equal to $\pi/2$, although the phase of the electromagnetic wave itself may not be definite.

In practice, much more often a situation occurs when transitions with a change in the projection of the angular momentum by both $+1$ and -1 are possible. For example, such a situation is realized when electrons with two spin values are present in the system, but their concentration differs, and the degree of spin polarization is determined by Eqn (1). Then, in accordance with the selection rules, both right- and left-polarized photons can be emitted, but their number, and therefore the intensity of right- and left-polarized electromagnetic waves, will differ. Such radiation is called partially circularly polarized in the literature [2, 18]. Quantitatively, partially circularly polarized radiation is described by the formula

$$P_{\mathrm{cp}} = \frac{I(\sigma^+) - I(\sigma^-)}{I(\sigma^+) + I(\sigma^-)} \times 100\% \,, \tag{24}$$

where $I(\sigma^+)$ and $I(\sigma^-)$ are the intensities of light with angular momentum $+1$ and -1, respectively, and P_{cp} is called the degree of circular polarization of light. Obviously, the degree of circular polarization is uniquely related to the degree of spin polarization of the charge carriers participating in recombination [19].

The value of P_{cp} varies from -100% to 100% (where -100% corresponds to the emission of photons whose electromagnetic field is right-hand circularly polarized, $+100\%$ corresponds to left-hand circularly polarized, and intermediate values $-100\% < P_{\mathrm{cp}} < 100\%$ correspond to radiation containing both components of circular polarization).

The concept of partially circularly polarized incoherent radiation should be explained. Recombination radiation, the degree of polarization of which is determined by Eqn (24), is not elliptically polarized, but, due to the action of conservation laws during carrier recombination, the properties of the radiation are such that, when using known polarization measurement schemes, the radiation will give a response corresponding to elliptically polarized light. However, in this case, due to the random nature of spontaneous optical transitions, the electromagnetic wave of electroluminescence radiation cannot be described by the mathematical model of elliptically polarized light.

In the simplest case of a two-level system (see Fig. 3) and holes with no spin polarization, the degree of circular polarization of light is equal to the degree of spin polarization of electrons:

$$P_{\mathrm{cp}} = P_n = \frac{n_+ - n_-}{n_+ + n_-} \times 100\% \,. \tag{25}$$

This is precisely the case frequently considered when analyzing the operation of spin light-emitting diodes.

The above principles of injection of spin-polarized charge carriers and emission of incoherent circularly polarized radiation during their recombination are realized in a device called a spin light-emitting diode [3]. Due to the electrical injection of charge carriers with a certain spin value from a magnetized ferromagnetic injector into a nonferromagnetic semiconductor of the spin LED, a nonequilibrium spin polarization of charge carriers is created in the latter. The injected spin-polarized carriers recombine with nonpolarized charge carriers of the opposite sign coming from the semiconductor, giving rise to partially circularly polarized radiation. The parameter characterizing the radiation is the degree of circular polarization (P_{cp}), which is defined by Eqn (24). Thus, in such a device, it is possible to specify one of two stable states, namely, right-hand and left-hand circular polarization of radiation. During analysis, the radiation behaves as circularly polarized; namely, in the classical detection scheme using a quarter-wave plate and a polarizer, the transmission of light depends on the relative position of the axes of the optical elements.

When developing the SLED, it was initially assumed that, due to the unambiguous relationship between the degree of circular polarization of electroluminescence and the degree of spin polarization of charge carriers, it would become an additional tool for studying the magnetic properties of some materials [20, 21]. But, as it turned out later, in addition to measuring magnetic properties, the use of SLEDs for transmitting spin information between spintronic devices is of interest. It is promising because light retains its circular polarization when propagating over long distances and, therefore, spin information can be transmitted over long distances as well. In addition, the advantages of this method of transmitting information include the elimination of heating losses associated with the motion of charge carriers, as well as the high speed of light propagation.

2.3 Detection of spin polarization of charge carriers in a semiconductor. Magnetoresistive element

Another method for detecting spin-polarized charge carriers injected into a nonferromagnetic layer is to use the magnetoresistance effect. This method was considered in early studies of spin injection [7]. It is based on the giant magnetoresistance (GMR) effect, which manifests itself in a change in the electrical conductivity of multilayer metal films

when changing the magnetization of ferromagnetic layers relative to each other in an external magnetic field. Parallel magnetization usually corresponds to a lower resistance than antiparallel magnetization. Spin injection from a magnetized ferromagnetic contact provides nonequilibrium spin polarization in the nonferromagnetic layer, and then, when carriers are extracted into the second ferromagnetic layer, the electrical resistance depends on the mutual orientation of the magnetizations. The high-resistance state is realized with antiparallel orientation, since the spins belonging to the 'majority' conductivity channel of the first magnetic layer will belong to the 'minority' conductivity channel in the second layer. With parallel orientation, the low-resistance state is realized [22–24].

To describe the giant magnetoresistance effect in multilayer films, the resistor model can be used [25, 26]. According to this model, all metal layers and all layer interfaces are considered to be resistors. For each spin channel, resistors are added in parallel or in series, depending on the ratio between the mean free path of charge carriers and the thickness of the metal layer. If the mean free path is small compared to the layer thickness, then each layer conducts electric current independently, which is equivalent to parallel-connected resistors. In this case, the resistances for parallel and antiparallel magnetizations are the same and, therefore, the amplitude of the giant magnetoresistance is zero. Hence, to obtain a nonzero GMR, the mean free path must be large enough. If the mean free path of electrons is much greater than the layer thickness, the scattering probability in a multilayer structure is the sum of the scattering probabilities in each layer and at each interface. Thus, for each spin channel, the resulting resistance can be represented as resistors connected in series. Let us consider a multilayer structure consisting of two ferromagnetic and two nonmagnetic layers (Fig. 4a, b). The directions of magnetization in the figures are indicated by thick arrows, and thin arrows are the trajectories of electrons flowing through two spin channels. It is assumed that the mean free path greatly exceeds the layer thickness, and the total electric current flows in the plane of the layers.

In ferromagnetic layers, the electron spin can be either parallel or antiparallel to the direction of magnetization, which corresponds to a carrier with a majority and minority spin. The values of resistance to currents with the majority ($\rho_\uparrow$) and minority ($\rho_\downarrow$) spin in the ferromagnetic layer are different, and the resistance of the bilayer consisting of a ferromagnetic and a nonmagnetic layer for each of the two ferromagnetic channels is equal to

$$R_{\uparrow,\downarrow} = \rho_N d_N + \rho_{\uparrow,\downarrow} d_F \,, \tag{26}$$

where ρ_N and d_N are the resistivity and thickness of the spacer (nonmagnetic) layer, and d_F is the thickness of the ferromagnetic layer. The resistance corresponding to the interface between the layers is omitted for simplicity. Equivalent circuits of the multilayer structure for the cases of parallel and antiparallel magnetization, presented in the form of resistors, are shown in Fig. 4c and 4d, respectively. For parallel magnetization, spin-up electrons pass through the structure almost without scattering, whereas spin-down electrons are extremely scattered inside both ferromagnetic layers. Since the conductivity is due to the parallel connection of two spin channels, the overall resistivity of the structure is low. For the antiparallel case, both spin-up and spin-down electrons are extremely scattered within one of the ferromagnetic layers, resulting in a high overall resistivity of the structure. The total resistance for the case of parallel magnetization can be expressed as

$$R_P = \frac{2R_\uparrow R_\downarrow}{R_\uparrow + R_\downarrow} \,. \tag{27}$$

The total resistance for the case of antiparallel magnetization is

$$R_{AP} = \frac{R_\uparrow + R_\downarrow}{2} \,. \tag{28}$$

Then, the value of magnetoresistance can be represented as

$$\frac{\Delta R}{R} = \frac{R_{AP} - R_P}{R_P} = \frac{(R_\uparrow - R_\downarrow)^2}{4R_\uparrow R_\downarrow} \,. \tag{29}$$

Equations (26) and (29) make it possible to reveal some regularities that determine the value of GMR. Let us assume that the resistance of nonmagnetic layers is less than the resistance of ferromagnetic layers; the expression for GMR then has the form

$$\frac{\Delta R}{R} = \frac{(\rho_\downarrow - \rho_\uparrow)^2}{4\rho_\downarrow \rho_\uparrow} = \frac{(\alpha - 1)^2}{4\alpha} \,, \tag{30}$$

where the spin asymmetry parameter $\alpha = \rho_\downarrow/\rho_\uparrow$ is introduced. According to Eqn (30), the value of giant magnetoresistance strongly depends on the difference in resistivity for the spin conduction channels in the ferromagnetic layers. To obtain high values of GMR, it is important to fulfill one of the conditions: $\alpha \gg 1$ or $\alpha \ll 1$. If there is no spin asymmetry for two conduction channels, i.e., $\alpha = 1$, then the giant magnetoresistance will be zero.

Next, it is necessary to consider the finite resistance of the nonmagnetic layer, which leads to the expression

$$\frac{\Delta R}{R} = \frac{(\alpha - 1)^2}{4(\alpha + pd_N/d_F)(1 + pd_N/d_F)} \,, \tag{31}$$

where $p = \rho_N/\rho_\uparrow$. From Eqn (31), it follows that, for a given value of α, the value of the GMR will increase with a decrease in the ratio pd_N/d_F. Thus, to obtain high GMR values, it is necessary to reduce the resistivity of the nonmagnetic layer ρ_N. With an increase in the thickness of the spacer layer d_N,

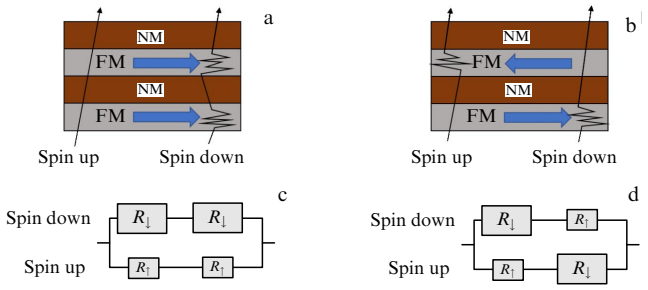

Figure 4. (a, b) Schematic diagram of a multilayer metal film, including nonmagnetic (NM) and ferromagnetic (FM) layers, magnetized parallel (a) and antiparallel (b). (c, d) Equivalent circuits of multilayer metal films, presented as resistors, for parallel (c) and antiparallel (d) magnetization of ferromagnetic layers.

the value of the giant magnetoresistance monotonically decreases.

Devices whose operation is based on the effect of giant magnetoresistance in magnetic multilayer structures have been the subject of numerous studies since their discovery in 1988 [27–29], which gave rise to the emergence of new technologies. The device developed based on the giant magnetoresistance effect was the magnetoresistive element. In this type of device, control of electrical resistance is implemented by changing an external magnetic field of a certain orientation. One of the design options of such a device is a spin valve, consisting of two layers of ferromagnet separated by a thin layer of nonmagnetic material. In one of the ferromagnet layers, the magnetic moment is 'fixed'; in other words, the magnetization of this layer is much less sensitive to changes in the external magnetic field (magnetically hard layer). Another ferromagnet layer is 'free' — its magnetization can be changed by applying a relatively weak external magnetic field (soft magnetic layer). If such layers are magnetized antiparallel, the resistance to electric current in such a structure will be high due to the additional contribution of spin-dependent scattering of spin-oriented carriers during transfer to a layer with opposite magnetization. If the layers are magnetized parallel, the resistance will decrease, since, with parallel magnetization of the carrier spins and the 'free' layer, the contribution of spin-dependent scattering is significantly reduced [27–30]. Based on this, in such a device, it is possible to set one of two stable states, namely, high and low resistance.

2.4 Combination of spin-dependent phenomena for constructing spintronic devices

The switching principle of both a magnetoresistive element and a spin light-emitting diode is used in information coding systems, in which information is represented as a binary code, a 'logical zero' and a 'logical one.' As a rule, a low signal level corresponds to a logical zero, and a high signal level, to a logical one. In microelectronics, the voltage on the element is used as a signal, and in optoelectronics, it is the intensity of optical radiation. In a magnetoresistive element, the signal is the voltage on the element, and in a spin light-emitting diode, it is the degree of circular polarization of optical radiation.

In Sections 2.1–2.3, we considered three basic spin-dependent effects, namely, spin injection from a magnetized electrode, radiative recombination with the participation of spin-polarized charge carriers, and the giant magnetoresistance effect. In the element base of spintronics, various devices implement one combination or another of these phenomena.

Magnetoresistive elements formed the basis of memory devices that allow for ultra-high recording densities [22–24]. Among the studies of magnetoresistive elements, one can distinguish Refs [31–33], in which the resistance of the system changes under the influence of a magnetic field, thus allowing such elements to be integrated into various systems, including magnetic field detection systems and display devices.

Recombination of spin-polarized carriers is used in spin light-emitting diodes that emit magnetically controlled circularly polarized light [34–37]. These devices are widely used, and detailed information about them is presented in the literature [3, 38]. In the cited papers, excitation of circularly polarized radiation occurs due to electrical injection of spin-polarized charge carriers from a ferromagnetic layer.

Note that most solutions published in the literature relate either to discrete devices or to the simplest integrated circuits implementing the high-density memory function. Of interest is further integration of the above-mentioned basic elements, which is a technological combination of various elements. This can significantly expand the functionality of spintronic devices and offer new solutions for information processing (coding, recording, transmission).

As far as we know, there are only a few publications on the technological combination of a magnetoresistive element (spin valve) and a light-emitting diode by creating an integrated circuit with a low degree of integration [39–43]. In these papers, the function of the magnetoresistive element is to control the total current (by switching the series resistance with an external magnetic field), which, in turn, controls the emission intensity of the LED. There are various design options for a magnetically controlled LED. In Refs [39, 40], integrated circuits with an electrical connection of two discrete devices are considered. In Ref. [41], the magnetoresistive element is a metal injection contact in a light-emitting diode. Also worth noting are Refs [42, 43] that report hybrid devices controlled by a magnetic field, which are a combination of inorganic magnetoresistive elements and organic light-emitting diodes with efficient electroluminescence.

Another way of integrating spintronic devices is the introduction of magnetic layers into the structure of a light-emitting diode to control the intensity of electroluminescence. Reference [44] reported the creation of a device in which an increase in the intensity of electroluminescence was obtained by applying an external magnetic field to it. Similar results were obtained in Ref. [45], where a magnetic material was built in a light-emitting device to change the flow path and distribution of the current density, as a result of which the efficiency of light emission was increased. It is also worth noting Ref. [46], where the built-in magnetic layer provided an increase in the efficiency of the light-emitting device due to the use of a magnetic field, holding electrons and holes in the active layer, which leads to an increase in the probability of recombination of electron–hole pairs.

The next stage of integration is the combination of a spin-injection device and a magnetoresistive element. No successful solution to this problem has been previously reported in the literature.

2.5 Samples for study and experimental technique

This paper reports the development of a laboratory prototype of a device emitting circularly polarized radiation with the ability to separately control the intensity and degree of circular polarization of the radiation by applying external magnetic fields. The device described in this paper is a magnetoresistive spin light-emitting diode (MR SLED), which is a combination of a semiconductor emitting heterostructure and a magnetoresistive element connected in series (the connection is implemented in an integrated design). The structure was formed in several stages. First, a semiconductor light-emitting heterostructure with an $In_{0.2}Ga_{0.8}As/GaAs$ quantum well (QW) was formed on an n-GaAs substrate by metalorganic chemical vapor deposition (MOCVD) under reduced pressure in a hydrogen flow. The depth of the quantum well occurrence was 120 nm. Upon completion of growth, the sample was removed from the reactor and transferred to the next technological operation. At the second stage, layers of the spin-polarized charge carrier injector of Al_2O_3 (1 nm), CoPd (8 nm), and Au (20 nm) were

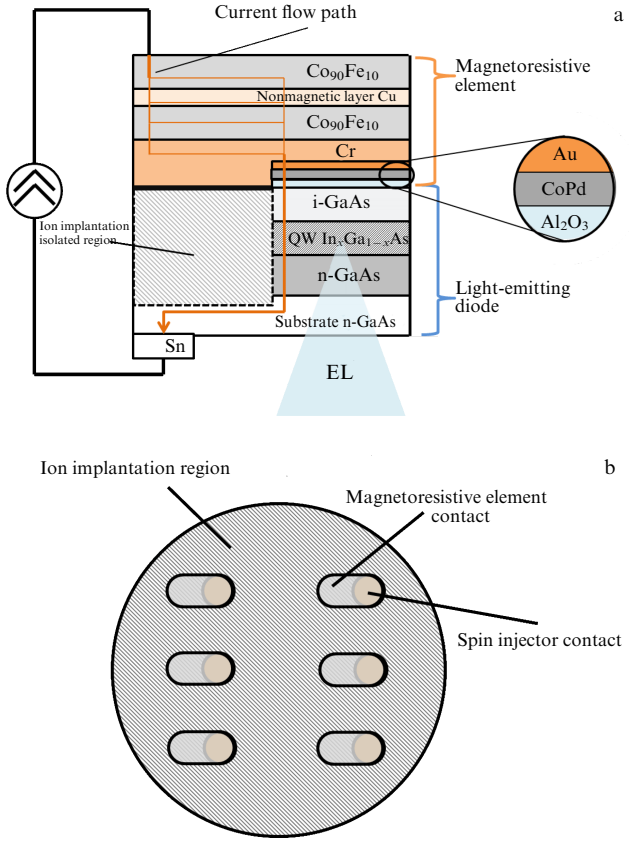

Figure 5. Schematic diagram of a magnetoresistive spin LED: (a) cross section and (b) top view.

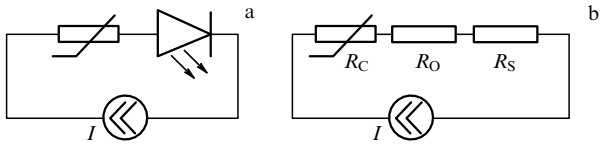

Figure 6. Connection diagram of integrated structure of magnetoresistive spin light-emitting diode: (a) schematic diagram, (b) equivalent circuit in forward bias mode.

successively deposited on the semiconductor heterostructure in another growth chamber using the electron–beam evaporation method in a vacuum. The Al_2O_3 layer formed on the surface of the light-emitting structure was tunnel-thin and was necessary to prevent diffusion of the ferromagnetic injector atoms into the semiconductor heterostructure and to ensure efficient spin injection from CoPd into the semiconductor. The ferromagnetic contact layer providing spin injection was a multilayer structure of 10 Co/Pd bilayers and had perpendicular magnetization anisotropy [47]. The Au layer served as a nonmagnetic interlayer to prevent exchange interaction between the ferromagnetic layers of the spin injector and the subsequent layers of the magnetoresistive element. In this way, a Schottky contact was formed based on the ferromagnetic metal/tunnel-thin dielectric/semiconductor system.

At the third stage, mesa structures (Fig. 5) were formed using photolithography and chemical etching. They were round metal contacts surrounded by a peripheral layer of a semiconductor electrical insulator. The peripheral layer of the insulator was formed by irradiating the regions of the GaAs semiconductor not covered by the Au contact with He^{++} ions (accelerating voltage $U = 40$ kV, fluence $D \sim 10^{14}$ cm^{-2}) which significantly increased its resistivity [48, 49].

At the fourth stage, a magnetoresistive element consisting of the following layers was grown on the surface of the formed diode mesa structures using electron beam evaporation in a vacuum: a Cr buffer layer (4 nm), a lower $Co_{90}Fe_{10}$ ferromagnetic layer (1.5 nm), a nonmagnetic Cu layer (3.7 nm), and an upper $Co_{90}Fe_{10}$ ferromagnetic layer (3 nm). To obtain the giant magnetoresistance effect, the thickness of the upper $Co_{90}Fe_{10}$ ferromagnetic layer differed from the thickness of the lower ferromagnetic layer. The layer thicknesses were chosen based on preliminary studies of the capabilities of the electron beam evaporation method, which showed that the greatest magnetoresistive effect is recorded exactly for these values.

Using lift-off lithography, mesa structures of a magnetoresistive element of a special shape were formed (Fig. 5b). At the final technological stage, a basic ohmic contact to the n-GaAs substrate was formed by spark firing-on of Sn foil. Figure 5 shows diagrams of a magnetoresistive spin light-emitting diode (a — sectional diagram, b — top view).

Control structures of the magnetoresistive element were also formed separately from the light-emitting diode. The structures were formed on an i-GaAs substrate and represented exactly the same sequence of layers as was formed at the fourth stage of the MR SLED technology.

Several measurements of electrical, magnetic, and optical characteristics were carried out with the manufactured structures. The measurements were carried out at a temperature of 10 K, maintained using a closed-cycle helium cryostat Janis CCS-300S/202.

Figure 6 shows the basic electrical circuit diagram of the connection of the formed integrated structure (Fig. 6a) and the equivalent circuit (Fig. 6b).

From the point of view of the electrical connection, the circuit is a magnetoresistive element and a spin light-emitting diode connected in series. This circuit was connected to a current source. Thus, a constant current I was passed through the elements, and the polarity of the voltage corresponded to the forward bias of the diode structure. With a reverse bias, the component associated with the high resistance of the reverse-biased diode dominates in the total resistance of the structure, so the relative amplitude of the resistance change was negligibly small. In this study, measurements of the voltage with a forward bias of the integrated structure were performed, as were measurements of the intensity and degree of circular polarization of the recombination radiation emitted with a forward bias of the spin light-emitting diode.

The most important design feature of the formed integrated structure is that the magnetoresistive layers cannot be considered a series-connected element. Such layers are part of the contact system that controls the currents of the majority and minority carriers through the metal/tunnel-thin dielectric/semiconductor structure [49]. A simplified equivalent electrical circuit of a magnetoresistive spin light-emitting diode in the forward bias mode is shown in Fig. 6b. It is the resistance of the metal contact to the spin light-emitting diode. The contact includes a magnetoresistive element, so the resistance value R_C depends on the applied magnetic field. The resistance R_O is the tunnel resistance of the dielectric layer Al_2O_3. In addition to the active part, the dielectric has a reactive component of resistance with a capacitance C_O, but, in the considered mode of constant electrical bias, the

capacitance does not contribute to the current flow processes. R_S is the resistance of the semiconductor, including the resistance of the depletion layer, which depends on the value of the applied electrical bias.

A series of measurements of the electric transport and electroluminescent characteristics was performed for the formed samples, including when placing the structures in an external magnetic field directed perpendicular to the plane of the structures and in the plane of the structures.

2.6 Measurements of magnetoresistive characteristics in a longitudinal magnetic field

To measure the magnetic field dependences of the static resistance of the integrated structure, the sample was placed in the gap of an electromagnet, the magnetic field being applied parallel to the plane of the structure. The magnetoresistance value was calculated using the following formula:

$$\mathrm{MR}(H) = \frac{R(H) - R(H_{\max})}{R(H_{\max})} \times 100\% \,, \tag{32}$$

where $R(H)$ is the resistance in the magnetic field H, and $R(H_{\max})$ is the resistance in the maximum applied magnetic field. We emphasize that the obtained value of $R(H)$ refers to the total resistance of the magnetoresistive element and the light-emitting diode, while, as will be shown below, in the forward bias mode, the resistance of the latter is relatively small.

2.7 Measurements of electroluminescence spectra of magnetoresistive spin light-emitting diodes

The electroluminescence spectra were measured to certify the diode part of the integrated structure. To measure the electroluminescence spectrum, a direct electric bias with respect to the base contact was applied to the upper ferromagnetic layer of the magnetoresistive element, which resulted in radiative recombination of carriers in the $In_{0.2}Ga_{0.8}As/GaAs$ QW. The light-emitting diode was powered in the pulsed current source mode. The current through the integrated structure varied within 36–50 mA. The radiation was extracted through the substrate of the magnetoresistive spin LED, which was transparent to the emitted radiation. The radiation was focused with a lens system onto the input of an MDR-23 monochromator and recorded by a silicon photodiode. The resulting signal, after being digitized and synchronized by the Stanford SR30 unit, was transmitted to a computer. Without applying a magnetic field, the magnetoresistive elements in the MR SLED circuit operate as a series resistance, setting the voltage drop across the diode structure [49]. The electroluminescence spectrum of the structures is shown in Fig. 7. The spectrum shows a peak at an energy of 1.26 eV, corresponding to the energy of the basic transition in a quantum well with a given $In_{0.2}Ga_{0.8}As/GaAs$ content.

2.8 Measurements of magnetic field dependence of electroluminescence intensity of magnetoresistive spin light-emitting diodes

When a magnetoresistive spin light-emitting diode is placed in an external magnetic field oriented in the plane of the layers, the resistance of the magnetoresistive element changes. With a constant current through the structure, this leads to a redistribution of voltages between the magnetoresistive element and the light-emitting diode. Ultimately, a change in the magnetic field leads to a modulation of the electroluminescence intensity of the LED. The efficiency of this process can be estimated by the relative change in the radiation intensity. The magnetic field dependence of the change in the relative EL intensity was calculated using the formula

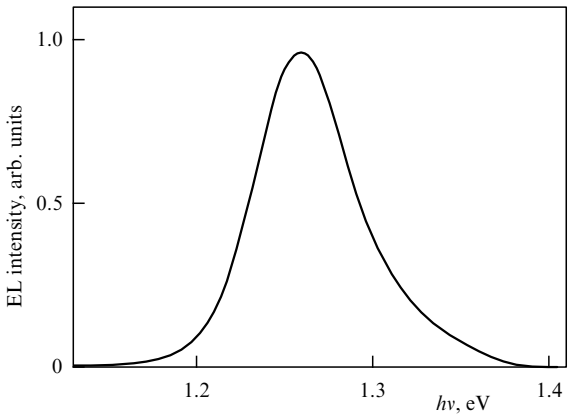

Figure 7. Electroluminescence spectrum of a magnetoresistive spin LED. Measurement temperature is 10 K, diode current is 38 mA.

$$I_{\mathrm{rel}}(H) = \frac{I(H) - I_0}{I_{\max}} \times 100\% \,, \tag{33}$$

where $I(H)$ is the relative EL intensity in the current magnetic field, I_0 is the relative EL intensity without applying a magnetic field, and $I_{\max}$ is the maximum value of the relative intensity in a magnetic field of $\sim \pm 500$ Oe.

The details of magnetically controlled electroluminescence measurements in a similar system are thoroughly described in Ref. [49].

2.9 Measurements of magnetic field dependences of degree of circular polarization of electroluminescence of formed structures

When a magnetoresistive spin LED is placed in an external magnetic field directed perpendicular to the surface of the structure layers, magnetization up to saturation of the CoPd ferromagnetic contact occurs. As a result, when a direct electric bias is applied, spin-polarized charge carriers are injected from the CoPd ferromagnetic contact into the active region of the light-emitting structure and recombine with the emission of partially circularly polarized radiation. By changing the polarity of the magnetic field to the opposite, it is possible to remagnetize the CoPd ferromagnetic contact and change the sign of the circular polarization. It should be noted that, since the CoPd film has an easy magnetization axis perpendicular to the surface of the layers, it is completely remagnetized in perpendicular magnetic fields greater than 0.1 T. On the contrary, magnetization of the structure perpendicular to the surface of the layers does not affect the magnetization of the layers of the magnetoresistive element in any way, since thin $Co_{90}Fe_{10}$ layers are characterized by an easy magnetization axis directed along the surface of the layers, and very strong magnetic fields (~ 1 T) are required for perpendicular magnetization of such layers. As a result, the LED will emit predominantly right- or left-handed circularly polarized radiation.

In this work, measurements of the magnetic field dependences of the degree of circular polarization of electro-

luminescent radiation (P_{cp}) were performed using the standard technique, a circuit diagram and description of which are given in Ref. [3]. Circularly polarized radiation of the quantum well was output through a substrate transparent to a given range in the direction of the magnetic field lines. A system of mirrors and lenses directed the plane-parallel beam through a quarter-wave plate and a Glan prism, after which it was focused on the entrance slit of the MDR-23 monochromator and recorded with a silicon photodiode. The quarter-wave plate was rotated, passing right- or left-circularly polarized radiation. The obtained readings of the photodiode were transmitted to a computer and saved for further processing. The values of the EL circular polarization degree were calculated using Eqn (24).

To improve the accuracy of measuring the characteristics, repeated studies of the samples were performed. The repeated measurements were performed in two modes:

— when connecting and continuously operating the diode, the recording of the magnetic field dependence of the intensity/degree of circular polarization was carried out 2 or 3 times;

— repeated measurements of diodes based on the same structures. In total, at least 10 diodes were manufactured based on each structure, and measurements were performed on at least three of them.

3. Experimental results and discussion

3.1 Current flow in integrated structure

Figure 8a shows the current-voltage characteristics (CVCs) of a magnetoresistive spin light-emitting diode measured in a zero magnetic field and with a longitudinal magnetic field of 250 Oe. Figure 8b shows the magnetic field dependence of the relative change in resistance of a magnetoresistive spin light-emitting diode measured at a temperature of 10 K with a current of 36 mA (the operating point is marked in Fig. 8a).

At a relatively small forward bias, the dominant contribution to the total resistance is made by the resistance of the semiconductor R_S. As the voltage increases, the resistance of the semiconductor decreases due to a decrease in the potential barrier and a decrease in the length of the space charge region. At voltage $U = \varphi_b/|e|$ (where φ_b is the height of the potential barrier in the Schottky diode), the potential barrier is completely straightened, the current–voltage characteristic becomes linear, and the resistance R_S becomes comparable to R_C and R_O, which is what is responsible for the detection of the effects considered below. In particular, when the structure is introduced into a longitudinal (directed along the surface of the structure layers) magnetic field, the slope of the characteristic in the linear section of the CVC changes, which is associated with an increase in the resistance of the magnetoresistive element (in accordance with Fig. 8b).

Note that, at lower voltages, the change in the CVC is imperceptible against the background of the very high resistance of the semiconductor. Thus, the magnetoresistive element affects the operation of the structure only in the mode of the light-emitting diode CVC rectification. It is in this mode that electroluminescence radiation is recorded in the diodes under study [37].

Let us consider in more detail the dependence of magnetoresistance on the magnetic field, measured in the linear region of the CVC. The plot shows two resistance maxima in a magnetic field of $\sim$ 340 Oe in absolute value. The

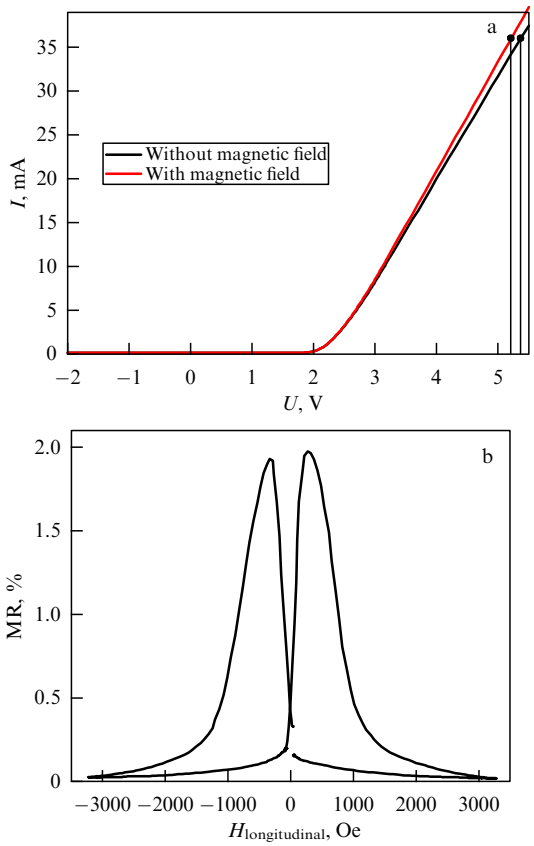

Figure 8. (a) Current–voltage characteristics of magnetoresistive spin light-emitting diode measured without magnetic field and with applied external longitudinal magnetic field of 350 Oe. Dots indicate current value at which magnetoresistive effect was measured. (b) Change in resistance in longitudinal magnetic field at current of 30 mA. Measurement temperature: 10 K.

maximum value of the resistance change for the device under study is $\sim$ 2%. The presence of maxima is due to the fact that the ferromagnetic layers of the magnetoresistive element differ in the value of the coercive field. When a positive magnetic field of sufficient magnitude (3000 Oe) is applied to the magnetoresistive element, the magnetization of both ferromagnetic layers of the MR element (soft and hard magnetic) becomes parallel. If the magnetic field is reduced to zero and a field of reverse polarity is applied and gradually increases, upon reaching 340 Oe, the magnetization of the soft magnetic layer will change to the opposite, so that the magnetization of the ferromagnetic layers of the magnetoresistive element will become antiparallel. As a result, when a current flows in such a structure, maximum resistance is observed due to the spin-dependent scattering of charge carriers. With a further increase in the magnetic field of reverse polarity, the magnetization of the hard magnetic layer also changes, due to which the magnetizations of both ferromagnetic layers of the magnetoresistive element become parallel.

3.2 Control of electroluminescence intensity

As noted above, the magnetoresistance affects electron transport in the forward bias region for which electroluminescence is recorded. Thus, magnetoresistance affects the operation of the light-emitting diode. Figure 9 shows the magnetic field dependence of the relative electroluminescence

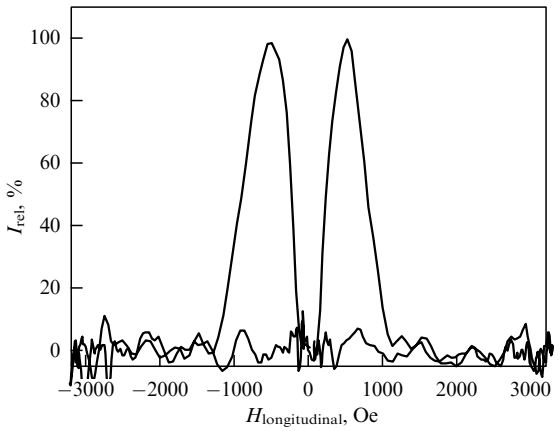

Figure 9. Dependence of relative EL intensity on longitudinal magnetic field. Measurement temperature: 10 K. Current through sample: 36 mA.

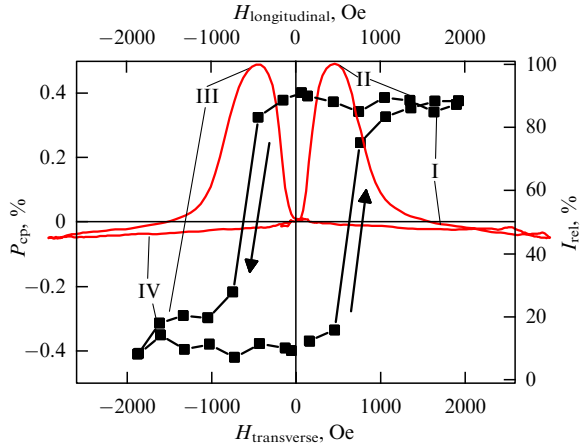

Figure 10. Dependences of degree of circular polarization P_{cp} on transverse magnetic field at zero longitudinal field (left) and EL intensity on longitudinal magnetic field at zero transverse field (right). Measurement temperature: 10 K. Current through sample: 38 mA.

intensity of the MR SLED measured at a temperature of 10 K and diode constant current of 36 mA. It is evident that the dependence is qualitatively like the magnetic field dependence of the magnetoresistance shown in Fig. 8b. This indicates control of the light-emitting diode intensity by switching the state of the magnetoresistive element.

Note that, in most studies devoted to magnetically controlled electroluminescence, the integrated circuit is connected to a voltage source [39–41]. In this case, the magnetoresistive element functions as a load resistor, the modulation of which makes it possible to change the current flowing through the structure. Since the emission intensity is controlled by the current, modulation of the total current leads to modulation of the intensity.

For the metal/tunnel-thin dielectric/semiconductor structures studied, a fundamentally different mechanism of electroluminescence is characteristic. This mechanism was considered earlier in a series of papers [50–53]. In accordance with the cited papers, the electroluminescence intensity is proportional not to the total current through the structure, but to the current of minority charge carriers (J_p), which, in turn, depends on the voltage drops at the resistors R_C and R_O,

$$I \sim J_p = \frac{2\pi m_h^* |e|^3}{h^3} \exp\left[-\frac{1}{h}(m_h^* \chi_h)^{1/2}\delta\right](U_C + U_O)^2 , \qquad (34)$$

where m_h^* is the effective mass of minority charge carriers (holes in the case under consideration), χ_h is the barrier value for holes in the dielectric, δ is the oxide thickness, and U_C, U_O are the fractions of the voltage drop across the metal and the tunnel-thin dielectric, respectively.

Note that, in the absence of a magnetoresistive element, the voltage drop across the metal (U_C) is negligibly small; therefore, in Refs [50–52], only the component of the voltage drop across the dielectric (U_O) is considered. In the structures under study, according to Eqn (34), an increase in the resistance of the magnetoresistive element in a magnetic field leads to an increase in J_p and a corresponding increase in the electroluminescence intensity.

In the current source mode,

$$J = J_p + J_e = \text{const} . \qquad (35)$$

Here, J_e is the current of the majority carriers (in this case, electrons).

At the current value J_p close to the threshold, but below it, no electroluminescence is detected without an external magnetic field. Due to the magnetoresistive effect in a magnetic field, the resistance of the magnetoresistive element increases, which leads to an increase in the voltage produced by the current source. With an increase in the total voltage, the voltage on all elements of the circuit increases, which leads to a decrease in the barrier for minority carriers and, thereby, to an increase in their current J_p to a value above the threshold, as a result of which electroluminescence radiation is recorded. It is this situation, in which the magnetoresistive element operates in the diode on/off mode, which is shown in Fig. 9. A decrease in the majority carrier current, accompanying an increase in J_p, does not have a significant effect on the EL intensity. A similar mechanism for increasing the electroluminescence intensity in a similar system is described in detail in Ref. [49].

With a current through the diode close to the threshold value (36 mA), varying the minority carrier current by means of the magnetoresistive effect makes it possible to change the EL radiation intensity by 100%, i.e., completely turn the LED on/off (see Fig. 9). In the low-resistance state, the minority carrier current is below the threshold value, so the EL intensity is zero; in the high-resistance state of the magnetoresistive element, the minority carrier current becomes higher than the threshold value, which allows EL to be recorded. When the current increases above the threshold value, electroluminescence radiation is recorded in both the low-resistance and high-resistance states of the magnetoresistive element; only the intensity values differ (red curve in Fig. 10). Thus, at a low current value, the MR SLED is controlled in the on/off mode; at an increased current value, the EL intensity varies. The dependence of the intensity on the current through the structure is considered in detail in Ref. [49].

It should be noted that the application of a transverse magnetic field to the structure does not allow the magnetoresistive element to be remagnetized. For this reason, the EL intensity remains unchanged in the entire range of values of a perpendicular magnetic field (±0.3 T).

3.3 Control of circular polarization degree of electroluminescence

When a magnetoresistive spin light-emitting diode is introduced into a magnetic field directed perpendicular to the surface, switching of the magnetizations of the magnetoresistive element layers does not occur, as shown above. Therefore, the perpendicular component of the magnetic field does not change the electroluminescence intensity. At the same time, in the range of magnetic fields used, magnetization up to saturation of the ferromagnetic contact CoPd is ensured. As a result, when a forward bias is applied to the device in a perpendicular magnetic field, injection of spin-polarized charge carriers from the ferromagnetic contact CoPd into the active region of the light-emitting structure and recombination with the emission of partially circularly polarized radiation occurs. By changing the polarity of the magnetic field to the opposite, it is possible to remagnetize the ferromagnetic contact CoPd and change the sign of the circular polarization. Thus, the LED emits predominantly right- or left-handed circularly polarized radiation. The value of the degree of circular polarization of the EL is calculated in accordance with relationship (24). The magnetic field dependence of the degree of circular polarization $P_{cp}(H)$ is shown in Fig. 10 (black curve).

It is evident that the magnitude of the degree of circular polarization P_{cp} nonlinearly depends on the magnetic field. In addition, a hysteresis loop is present on the dependence $P_{cp}(H)$. The magnitude of the coercive force is ~ 700 Oe. The maximum value of P_{cp} is 0.4%. When a longitudinal magnetic field is applied to the structure, the value of P_{cp} remains unchanged in the field range used.

Figure 10 illustrates the summary result of studies on a magnetoresistive spin light-emitting diode. The figure shows the superposition of the dependences of the EL intensity on the longitudinal magnetic field (see Fig. 9) and the degree of circular polarization on the transverse magnetic field. The Roman numerals indicate the possible states of the device: I — right circular polarization with low radiation intensity, II — right circular polarization with high radiation intensity, III — left circular polarization with high radiation intensity and IV — left circular polarization with low radiation intensity. The diode can be in each of these states for a long time (up to several days) while maintaining the required values of the magnetic field (~ 450 Oe for the longitudinal field controlling the intensity, and 0 Oe for the transverse field controlling the circular polarization).

Note that, for simultaneous recording of the intensity and circular polarization of electroluminescence in all states of the magnetoresistive element, the current through the sample must exceed the threshold value, but the total change in intensity must be less than 100%. This is just the mode shown in Fig. 10: the diode current is more than 36 mA (38 mA). The maximum change in intensity in this case was 60%.

The proposed scheme is comparable in electroluminescence intensity to similar light-emitting diodes [53], but is inferior in the maximum value of the degree of circular polarization (see, e.g., [3, 18]). We emphasize that, in publications devoted to measurements of circularly polarized electroluminescence, the radiation intensity is not analyzed, and polarization characteristics are not studied when analyzing light-emitting diodes. A special feature of the structure studied is the possibility of simultaneous variation of both the intensity and circular polarization of light. From a practical point of view, the fundamental demonstration of a magnetoresistive spin light-emitting diode in four stable states can be used for wireless magnetometry, as well as for recording and transmitting information. Usually, binary coding is used in spintronics, in which the device is in one of two stable states. The structure studied makes it possible to implement a quaternary system in which each of the four states can be maintained for a sufficiently long time, and the possibility of circularly polarized emission ensures the transmission of recorded information by means of intensity and circular polarization of light. This will provide a twofold increase in information capacity without changing the area of the structure.

4. Conclusion

In this paper, we consider the fundamental physical principles underlying the operation of the basic elements of spintronics: the magnetoresistive effect, the injection of spin-polarized charge carriers from a magnetized ferromagnetic electrode, and the radiative recombination involving spin-polarized carriers. An integrated structure implementing all the above phenomena, a magnetoresistive spin light-emitting diode, has been manufactured and investigated. The structure is a series-connected magnetoresistive element and a spin light-emitting diode based on a metal/tunnel-thin dielectric/semiconductor system in a microscale integrated design. It is shown that an external magnetic field directed in the plane of the layers makes it possible to modulate the resistance of the magnetoresistive element (high or low resistance) and thereby control the intensity of the diode electroluminescence. The magnetic field directed perpendicular to the plane of the layers provides magnetization of the magnetic contact of the spin light-emitting diode and spin injection, accompanied by the emission of circularly polarized light. As a result, a device is formed that can be in four stable magnetic states (high–low intensity, 'positive'–'negative' circular polarization), which seems promising for the circuit design of digital optoelectronics.

The study was supported by the Russian Science Foundation, project no. 21-79-20186.

References

1. Žutić I, Fabian J, Das Sarma S *Rev. Mod. Phys.* **76** 323 (2004)
2. Meier F, Zakharchenya B P (Eds) *Optical Orientation* (Modern Problems in Condensed Matter Sciences, Vol. 8) (Amsterdam: North-Holland, 1984); Zakharchenya B P, Meier F (Eds) *Opticheskaya Orientatsiya* (Optical Orientation) (Leningrad: Nauka, 1989)
3. Holub M, Bhattacharya P *J. Phys. D* **40** R179 (2007)
4. Sinova J et al. *Rev. Mod. Phys.* **87** 1213 (2015)
5. Nagaosa N et al. *Rev. Mod. Phys.* **82** 1539 (2010)
6. Kudrin A V et al. *Phys. Rev. B* **90** 024415 (2014)
7. Datta S *Nat. Electron.* **1** 604 (2018)
8. Sato S, Tanaka M, Nakane R *Phys. Rev. B* **102** 035305 (2020)
9. Islam Md E, Hayashida K, Akabori M *AIP Advances* **9** 115215 (2019)
10. Dyakonov M I, cond-mat/0401369; in *Future Trends in Microelectronics: the Nano, the Giga, and the Ultra* (Eds S Luryi, J Xu, A Zaslavsky) (Hoboken, NJ: Wiley, 2004) p. 157
11. Awschalom D D, Flatté M E *Nature Phys.* **3** 153 (2007)
12. Yadav M K et al. *Mater. Sci. Eng. B* **303** 117293 (2024)
13. Maekawa S (Ed.) *Concepts in Spin Electronics* (Ser. on Semiconductor Science and Technology, Vol. 13) (Oxford: Oxford Univ. Press, 2006)
14. Aronov A G, Pikus G E *Sov. Phys. Semicond.* **10** 698 (1976); *Fiz. Tekh. Poluprovodn.* **10** 1177 (1976)

15. Young D K et al. *Semicond. Sci. Technol.* **17** 275 (2002)
16. Crooker S A et al. *Science* **309** 2191 (2005)
17. Yur'ev Yu V *Svetovye Volny i Fotony* (Light Waves and Photons) (Moscow: MFTI, 2010)
18. Salis G et al. *Appl. Phys. Lett.* **87** 262503 (2005)
19. Lampel G *Phys. Rev. Lett.* **20** 491 (1968)
20. Fiederling R et al. *Nature* **402** 787 (1999)
21. Ohno Y et al. *Nature* **402** 790 (1999)
22. Ennen I et al. *Sensors* **16** 904 (2016)
23. Dagotto E *Nanoscale Phase Separation and Colossal Magnetoresistance*: *the Physics of Manganites and Related Compounds* (Springer Ser. in Solid-State Sciences, Vol. 136) (Berlin: Springer-Verlag, 2003) https://doi.org/10.1007/978-3-662-05244-0
24. Tian Y, Yan S *Sci. China Phys. Mech. Astron.* **56** 2 (2013)
25. Edwards D M, Mathon J, Muniz R B *IEEE Trans. Magn.* **27** 3548 (1991)
26. Mathon J *Contemp. Phys.* **32** 143 (1991)
27. Sato H et al. *Superlatt. Microstruct.* **4** 45 (1988)
28. Baibich M N et al. *Phys. Rev. Lett.* **61** 2472 (1988)
29. Binasch G et al. *Phys. Rev. B* **39** 4828 (1989)
30. Bruno P *Phys. Rev. B* **49** 13231 (1994)
31. Milyaev M A, Naumova L I, Ustinov V V *Phys. Met. Metallogr.* **119** 1162 (2018); *Fiz. Met. Metalloved.* **119** 1224 (2018)
32. Sharko S A et al. *J. Alloys Compd.* **846** 156474 (2020)
33. Chung K H, Kim S N, Lim S H *Thin Solid Films* **650** 44 (2018)
34. Hanbicki A T et al. *Appl. Phys. Lett.* **80** 1240 (2002)
35. Oh E et al. *J. Appl. Phys.* **106** 043515 (2009)
36. Liang S H et al. *Phys. Rev. B* **90** 085310 (2014)
37. Baidus N V et al. *Appl. Phys. Lett.* **89** 181118 (2006)
38. Mustaqeem M et al. *Adv. Funct. Mater.* **33** 2213587 (2023)
39. Appelbaum I et al. *Appl. Phys. Lett.* **83** 4571 (2003)
40. Saha D, Basu D, Bhattacharya P *Appl. Phys. Lett.* **93** 194104 (2008)
41. Kudrin A V et al. *Tech. Phys. Lett.* **37** 1168 (2011); *Pis'ma Zh. Tekh. Fiz.* **37** (24) 57 (2011)
42. Sun D et al. *Appl. Phys. Lett.* **103** 042411 (2013)
43. Sun D et al. *SPIN* **4** 1450002 (2014)
44. Takeshi M ''Magnetic-infrared-emitting diode'', Patent US-4450460-A (2008)
45. Xuan R et al. ''Light emitting device within magnetic field'', Patent WO2009089739A1 (2009)
46. Tae L W et al. ''Semiconductor light-emitting device'', Patent US-10636940-B2 (2015)
47. Dorokhin M V et al. *Ann. Physik* **536** 2300480 (2024)
48. De Souza J P, Danilov I, Boudinov H *Appl. Phys. Lett.* **68** 535 (1996)
49. Ved M et al. *Appl. Phys. Lett.* **118** 092402 (2021)
50. Livingstone A W, Turvey K, Allen J W *Solid-State Electron.* **16** 351 (1973)
51. Card H C, Rhoderick E H *Solid-State Electron.* **16** 365 (1973)
52. Card H C, Smith B L *J. Appl. Phys.* **42** 5863 (1971)
53. Dorokhin M V et al. *J. Surf. Investig.* **4** 390 (2010); *Poverkhnost Rentgen. Sinkhron. Neitron. Issled.* (5) 34 (2010)